Final Draft
of the original manuscript:

Steinhilber, D.; Sisson, A.L.; Mangoldt, D.; Welker, P.; Licha, K.; Haag, R.:
Synthesis, Reductive Cleavage, and Cellular Interaction Studies of Biodegradable, Polyglycerol Nanogels
In: Advanced Functional Materials (2010) Wiley

DOI: 10.1002/adfm.201000410

Submitted to ADVANCED FUNCTIONAL MATERIALS

DOI: 10.1002/adfm.((please insert DOI)

Synthesis, Reductive Cleavage, and Cellular Interaction Studies of Biodegradable, Polyglycerol Nanogels

By *Dirk Steinhilber, Adam L. Sisson*, *Dorothea Mangoldt*, *Pia Welker, Kai Licha,* and *Rainer Haag**

Dedicated to Professor George Whitesides on the occasion of his 70th birthday

[*] Prof. R. Haag, D. Steinhilber
Institute for Chemistry and Biochemistry
Free University Berlin
Takustrasse 3, Berlin 14195 (Germany)
E-mail: haag@chemie.fu-berlin.de
Dr. A. L. Sisson
GKSS Forschungszentrum Geesthacht
Institute for Polymer Research
Kantstrasse 55, Teltow-Seehof 14513 (Germany)
Dr. P. Welker, Dr. K. Licha
mivenion GmbH
Robert-Koch-Platz 4, Berlin 10115 (Germany)

Keywords: Stimuli-responsive materials, polymeric materials, polyglycerol nanoparticles, hydrogels, biomedical applications

In this paper we describe disulfide containing, polyglycerol nanogels as a new class of biodegradable materials. These nanoparticles are prepared in inverse miniemulsion via an acid catalyzed ring-opening polyaddition of disulfide containing polyols and polyepoxides. Varying conditions allow us to tune particle size and disulfide content within the polymer network; particles can be prepared with narrow polydispersities with diameters in the range from 25 to 350 nm. Particle degradation under reductive intracellular conditions is studied by various analytical techniques. Gel permeation chromatography indicates that final degradation products have relatively low molecular weights (≤ 5 kDa). In addition, studies in cell culture show these nanoscale materials to be highly biocompatible. Dye-labelled nanogels are shown by optical microscopy techniques to readily internalize into cells by endocytotic mechanisms. This study highlights the great potential of these particles to function as sophisticated nanotransporters that deliver cargo to a certain tissue or cell target and then biodegrade into

smaller fragments which would be cleared from the body by the kidney. (with ~ 30 kDa molecular weight cut off)

1. Introduction

Multifunctional and biodegradable polymeric nanoparticles for drug or dye delivery are of crucial importance for many biomedical applications.[1-3] Nanogels (sometimes referred to in the literature as microgels) are high molecular weight polymers with characteristics of both dendritic and macroscopically cross-linked materials. Nanogels typically result when polymerization between multifunctional monomers is carried out in an enclosed volume (emulsion, micelle etc.).[4-7] Sizes are tunable by various techniques from the low nanometer to the micrometer range. A particular concept to produce sophisticated materials is to introduce biodegradable or bioresponsive elements within polymeric structures. Biodegradable functionalities sensitive to proteases (peptides),[8-10] or to pH (esters,[11,12] carbonates,[13] and acetals,[14,15]) have been incorporated within nanogels. Polyesters of α-hydroxycarboxylic acids such as poly(lactide-*co*-glycolide) are widely studied and utilized in the preparation of biodegradable materials.[16,17]

Neutral nanoparticles (≥ 10 nm) are known to internalize within cells by endocytic mechanisms.[3] The use of redox labile disulfide bonds as biodegradable linkers is a promising approach to achieve post-endocytic nanoparticle degradation.[18] Lysosomes contain reductive enzymes that maintain an approximate 5 mM concentration of the thiol containing tripeptide reducing agent glutathione.[19] Disulfide bonds are typically stable in the largely oxidative extracellular media therefore site specific cleavage of internalized nanoparticles and possible release of active agents to the cytoplasm should be possible. Of particular interest, Matyjaszewski and co-workers have prepared disulfide containing nanoparticles and shown them to be cleaved efficiently under reducing conditions.[20] Doxorubicin was loaded within

such particles, only being released and showing in vitro cytotoxicity, when glutathione was added.[21]

Highly branched polyglycerols are a class of highly biocompatible polyether-polyols[22,23] with a globular dendritic structure. Hyperbranched polyglycerols are typically prepared by ring opening polymerization of glycidol either by cationic[24,25] or anionic[26,27] means. There are a number of polyglycerol materials being used in many biomedical applications.[28] We have prepared biodegradable hyperbranched polyglycerols with pH responsive linkers within our group and studied the tumor tissue uptake of drugs and dyes in vivo.[29,30] One drawback, however, is that traditional synthetic techniques only afford polymers with a maximum size of approximately $M_n \approx 1$ MDa (diameter ≈ 10 nm).[31] Based upon increased insights into the mechanisms of nanoparticle endocytosis,[32] we hypothesize that the optimum size for nanoparticle endocytic uptake into cells would be a diameter in the range of 25 - 100 nm. Consequently, we recently developed the preparation of biocompatible polyglycerol based nanogels in the desired size range that exhibit efficient cell penetration properties by endocytic means.[33]

Here we describe methods to prepare biodegradable nanogels with controllable dimensions with a disulfide-linked polyglycerol structure. These nanoparticles are stable under typical physiological conditions but efficiently break down into smaller segments under reducing intracellular conditions. The twofold benefit of such environment responsiveness is that such polymers should be cleaved with possible drug release within reductive cell compartments (e.g. lysosomes); following cleavage, the less toxic and smaller fragments are produced that can be cleared by the kidneys.

2. Results and Discussion

2.1. Synthesis of Degradable Polyglycerol Nanogels

Our approach to degradable polyglycerol nanogels is based on acid catalyzed miniemulsion polymerization. Miniemulsions are special heterophase dispersions of relatively stable nanodroplets in a continuous non-solvent phase.[34] Narrowly size distributed droplets in the range 20 - 200 nm result from a high shearing of the biphasic system in the presence of an appropriate surfactant. Each droplet behaves as a discrete nanoreactor and a whole range of polymerization reactions can be initiated within, to lead to size defined products. Our system is based upon an *inverse* miniemulsion system wherein the polar reactants are dispersed in non-polar cyclohexane. A poly(ethylene-*co*-butylene)-*block*-poly(ethyleneoxide) surfactant was found to act as an excellent stabilizer of polar nanodroplets,[35] particularly if a small amount of dimethylsulfoxide is mixed in to suppress Ostwald ripening droplet destabilization.[36] Miniemulsions were formed by ultrasonication with a sonic tip prior to addition of para-toluenesulfonic acid (PTSA) catalyst. Monomers used were varying mixtures of glycerol **1**, glycerol tris-glycidyl ether **2** and disulfide-derivatives **3**,[37] and **4**,[38] as shown in Scheme 1. Readily dispersible or soluble products were formed with relatively narrow size distribution (Table 1).

Initially, disulfide containing polyglycerol nanogels were formed by combining glycerol tris-glycidyl ether **2** and bis-3-thioglycerol disulfide **3** under acid catalyzed polyaddition conditions. Sizes of the obtained products **5a-d** could be rationally controlled by varying the concentration of DMSO in the polar dispersed phase, relative to the concentration of monomers. Dispersed phase droplets which were more dilute in monomers gave smaller products, as has been previously observed within our group.[39] Sizes could be varied between ≈ 90 and 350 nm in diameter. However, solubility in aqueous media was limited in such

systems. Particles **5a-d** could be dispersed with some agitation to give turbid suspensions which showed precipitation behavior after a period of approximately 24 - 48 h. In order to increase hydrophilicity and so obtain full aqueous solubility, glycerol **1** was added as a co-monomer to replace a fraction of the substantially more hydrophobic bis-3-thioglycerol disulfide **3.** This way soluble nanogels **5e-f** were obtained with a relatively smaller size, between ≈ 60 and 95 nm. The addition of polar glycerol seemed to reasonably stabilize the formation of smaller nanoreactors upon miniemulsification. The downside of this approach is that the fraction of disulfide linkages in the final nanoparticle relative to the non-labile ether linkages is reduced, which might lead to reduced degradabilities. Therefore an alternative approach was developed wherein the disulfide linkage was incorporated into the hydroxyethyldisulfide-bis-glycidylether **4** which was cross-linked with glycerol **1** following the same protocol to give freely soluble hydrophilic nanogels **5g** with a high proportion of disulfide crosslinks and a particle size ≈ 25 nm.

2.2. Nanogel Degradation Studies

The turbidity of products **5a-d** could be used to study the degradation of such nanoparticles in a reducing environment. A degassed suspension of 10 mg of particles **5d** in phosphate buffered saline (PBS; pH 7.4) buffer was treated under argon with a 1:1 w/w quantity of the bis-thiol reducing agent dithiothreitol (DTT),[40] and subsequent particle degradation was followed by using a UV-vis turbidity assay. As can be seen in Figure 1a, before DTT addition a turbid dispersion in PBS was clearly visible with reduced transmission in the UV-vis as a result of light scattering as it passed through the sample. Upon DTT addition a rapid visible increase in transmission, quantified by UV-vis spectroscopy was detected. This is a result of the nanoparticles being degraded into lower molecular weight

fragments that are either totally soluble in the buffer or too small to scatter light in the UV-vis region.

Reductive degradation was also followed by analysing samples at time intervals using gel permeation chromatography. To aid detection with the UV-vis reader of the GPC instrument samples were labelled with fluorescein isothiocyanate (FITC) through thiocarbamate linkage (see Supporting Information).[41] Undegraded nanogels had a retention volume of approximately 40 ml, which is deemed to be around the solvent front of the particular apparatus setup (1 MDa upper retention limit). As can be seen in Figure 1b, reaction of **5f-FITC** in PBS buffer with DTT (50 mM) gave products after 18 h which exhibited substantially greater retention to the column. After the prolonged reaction time of 64 h marginally greater retention was observed but longer reaction times had negligible effect, which lead to the hypothesis that complete degradation had occurred earlier. By comparison with the mean retention times of known lower molecular weight FITC labelled polyglycerol samples prepared routinely in our group,[42] it can be inferred that these degraded fragments have a molecular weight in the region of ≤ 5 kDa. The same sample was likewise analyzed to investigate degradation under simulated intracellular conditions with glutathione as reducing agent (PBS buffer, 37 °C, 5 mM glutathione). Although these conditions are relatively mild compared to those previously described, significant degradation was observed after 24 h and with prolonged reaction times fragments with an estimated molecular weight < 5 kDa were exclusively obtained. It should be noted that the renal clearance threshold for macromolecules, below which excretion via the kidney becomes effective, is estimated to be in the order of 30 kDa.[43,44]

DTT mediated nanoparticle degradation was also followed by employing a dialysis assay. Indodicarbocyanine (IDCC) dye loaded nanogels **5g•IDCC**[45] were prepared by conducting miniemulsion polymerization in the presence of the hydrophilic fluorophore

(Supporting Information). Nanogel **5g•IDCC** was subsequently dissolved in PBS buffer and placed in a dialysis tube (molecular weight cutoff = 1,000 Daltons, pore size approximately 1-2 nm). Dialysis was conducted against a 50 mM DTT solution in PBS over 7 d with changing of the external solution 3 times per day. Gradual leakage of unencapsulated dye from the dialysis tube was observed by measuring the fluorescence signal of aliquots of the solution inside the dialysis tube. Figure 1c) shows how fluorescence from within the tube decreased over time. This is attributed to reductive degradation of the nanogels into smaller fragments with concomitant release of the entrapped dye. In a control experiment, negligable decrease in fluorescence was recorded when **5g•IDCC** was dialysed against PBS buffer in the absence of DTT. Although our near infra-red IDCC dye is colorless to the naked eye, this phenomenon could be observed visually when Fluorescein (Fl) loaded nanogels **5g•Fl** were treated in the same manner. Figure 1 shows a dialysis experiment in which **5g•Fl** has been dialysed against PBS for 2 d in the presence of DTT (Fig. 1e)); and in the absence of DTT (Fig. 1f)).

2.3. Nanogel Interactions with Cells

In our previous communication, we showed that non-degradable polyglycerol nanogels are able to rapidly endocytose in vitro.[33] Likewise, fluorescence microscopy was used to study the uptake kinetics of rhodamine B isothiocyanate (RITC)-conjugated biodegradable polyglycerols **5g-RITC** into human lung cancer A549 cells. Cell culture was incubated with nanogels at 37 °C and samples were analyzed at set time intervals. Figure 2 shows the time dependent uptake of **5g-RITC**, with rapid internalization starting within 30 min and visibly increasing over time until a plateau was reached at 4 h. The low molecular weight RITC labelled glycerol control showed no uptake. With nanogel mediated dye uptake, some localized regions of high intensity were observed, which are expected to correspond to endocytotic vesicles (see also Supporting Information).

We aimed for further insight into endocytotic pathways and intracellular locations of the nanogels **5g-RITC**, by specific staining the late endosomes with commercial green fluorescing antibodies. The studies depicted in Figure 2f)-h) show that nanogels **5g-RITC** located after 1h incubation time numerously in late endosomes, which are assembled in the perinuclear region. Interestingly one can also identify nanogels (red signal in Figure 2h)) outside the endocytic vesicles which indicates that they have escaped from the endosomes.

In order to show intracellular biodegradation, we compared the cellular uptake kinetics of the disulfide containing nanogels **5g-RITC** with the previously reported stable polyglycerol nanogels,[33] by fluorescence activated cell sorting (FACS). Starting from the same fluorescence intensities after 2 h, the cells, which were incubated with stable polyglycerol nanogels, show an almost doubled fluorescence compared to the degradable analogues **5g-RITC** after 24 h incubation time (figure 3a)). This phenomenon can be explained by intracellular reduction of the nanogels **5g-RITC** and subsequent faster cell clearance of the degraded fragments compared to the stable polyglycerol nanogels. It is noteworthy that this difference between biodegradable and non-biodegradable nanogels is glutathione dependent. Glutathione inhibition experiments show that the biodegradable nanogels show similar cell fluorescence compared to the non-degradable nanogels (see Supporting Information). Therefore we conclude that the new biodegradable nanogels are actually degraded inside the cells by disulfide reduction to smaller polyglycerol fragments as clearly demonstrated by the in vitro experiments shown in figure 3.

Biocompatibility of these materials was probed by selecting nanogel **5e** as a test compound and investigated effects on human hematopoietic U-937 cell proliferation (cell number), viability, and metabolic activity (MTT test). Experiments were carried out in 10% fetal calf serum and conducted at varying concentrations of **5e**. Pure buffer was used as control and apoptosis-inducing dexamethasone (Dex; toxic at 10^{-5} M; 0.004 mg/ml) was used

as a negative control. A high concentration of **5e** was necessary to promote adverse affects (10^{-6} M; 5.0 mg/ml); this figure is comparable to that of our non-degradable polyglycerol nanogels as highlighted with MTT tests in Figure 3. However, together with its biodegradability, the new carrier systems should be tolerated better due to possible kidney clearance (kidney cutoff approx. 30 kDa). Further details are described in the Supporting Information section. These highly biocompatible materials exhibited minor interaction with biological structures.

3. Conclusions

In summary, we have expanded our polyether miniemulsion chemistry to biodegradable polyglycerol nanogels with promising transport properties for cellular delivery. A simple one- step process was developed and conditions were tuned to vary particle size and nanogel composition. A variety of polyols and polyepoxides, which led to new functional materials, could be polymerized following our general procedure. These disulfide containing nanogels were degraded into small oligomeric subunits in reducing environments, as shown by three different assays in this publication. Furthermore, disulfide containing polyglycerol nanogels were found to be highly biocompatible, much the same as non-degradable polyglycerol based nanogels. Our studies show that these materials are able to rapidly enter cells by endocytic mechanisms, thus entering the reductive intracellular environment. One main goal is to use these constructs as sophisticated nanovehicles that deliver a cargo to a certain tissue or cell target and then biodegrade into rapidly cleared fragments that can be cleared by the kidneys. Further studies on drug/dye encapsulation, surface functionalization (e.g. with cell targeting ligands), and the endocytic mechanism and fate of internalized nanogels are ongoing.

4. Experimental

Materials: General chemicals were purchased from Acros Organics and used reagent grade; DMSO was used in extra dry form and purchased from Sigma Aldrich. Cyclohexane was obtained from ROTH, thioglycerol and dibutyltin dilaurate was purchased from Sigma Aldrich. Commercial glycerol-tris-glycidylether (GE 100) was received as a kind gift from Raschig GmbH and the block-co-polymer surfactant poly(ethylene-co-butylene)-block-poly(ethyleneoxide) [34], was received as a kind gift from Helmut Schlaad (Max Planck Institute for Colloids & Interfaces, Golm, Germany).

Bis-3-thioglycerol disulfide was synthesized following the literature procedure [37]. Hydroxyethyldisulfide-bis-glycidylether was synthesized following the literature procedure [38]. Emulsions were sonicated using a sonicator, W-220f, with microtip on 70% intensity (Heat Systems Ultrasonics, Inc.) Dynamic light scattering measurements were conducted using a BioDLS particle sizer (Brookhaven Instruments Corp.). ^{1}H NMR spectra were recorded on a Bruker AC250 at 250 MHz. Deuterated methanol and deuterated chloroform were used as solvents for NMR experiments. Size Exclusion Chromatography (SEC) measurements were performed on PSS Suprema columns (serial connection of 100Å, 100-100000 Da; 1000 Å, 100-1000000 Da; and 3000 Å, 100-3000000 Da) in Phosphate Buffered Saline (pH 7.4) as eluent, UV-vis detector set on 450 nm, flow rate 1 mL/min. Dialysis (benzoylated cellulose dialyse tubes, *SIGMA-ALDRICH*, (MWCO) = 1000 g·mol^{-1}) in PBS buffer was performed in a 1 L beaker, changing the solvent 3 times over a period of 24 h.

General procedure for the preparation of the nanogels ***5a-5g***: Solutions of poly(ethylene-*co*-butylene)-*block*-poly(ethyleneoxide) surfactant in cyclohexane and monomers **1-4** in DMSO were prepared (amounts were varied according to Table 1). After

mixing, the sample was pre-emulsified under vigorous magnetic stirring for 1 h. The formed macroemulsion was ultrasonicated (SonicatorTM, W-220f, Microtip, 70% intensity, heat systems ultrasonics, Inc.) four times for one minute under ice cooling. The white and milky emulsion was further magnetically stirred and after addition of 10 mg of PTSA the reaction mixture was heated to 115 °C in a sealed tube for 16 h. The remaining epoxide functionalities were quenched by addition of water and further stirring of the reaction mixture at 115 °C for 6 h. The product was isolated by addition of n-hexane to the emulsion and centrifugation (4000 min^{-1}, 10 min). This procedure was repeated 3 times to remove remaining surfactant. After solvent evaporation, a highly viscous product was obtained. Remaining unreacted monomer was removed by dialysis in water (products **5e-5g**) and ethanol (**5a-5d**).

Acknowledgements

We thank the German Science Foundation (SFB 765) for funding and the Alexander von Humboldt Foundation for financial support to A.L.S., Michael Staegemann for synthetic support, and Helmut Schlaad for surfactant donation. ((Supporting Information is available online from Wiley InterScience or from the author)).

Received: ((will be filled in by the editorial staff))
Revised: ((will be filled in by the editorial staff))
Published online: ((will be filled in by the editorial staff))

_[1] J. Panyam, V. Labhasetwar, *Adv. Drug Del. Rev.* **2003**, *55*, 329.

_[2] S. Nayak, L. A. Lyon, *Angew. Chem. Int. Ed.* **2005**, *44*, 7686.

_[3] A. Prokop, J. M. Davidson, *J. Pharm. Sci.* **2008**, *97*, 3518.

_[4] M. Antonietti, *Angew. Chem. Int. Ed. Engl.* **1988**, *27*, 1743.

_[5] M. Das, H. Zhang, E. Kumacheva, *Annu. Rev. Mater. Res.* **2006**, *36*, 117.

_[6] J. K. Oh, R. Drumright, D. J. Siegwart, K. J. Matyjaszewski, *Prog. Polym. Sci.* **2008**, *33*, 448.

_[7] A. V. Kabanov, S. V. Vinogradov, *Angew. Chem. Int. Ed.*, **2009**, *48*, 5418.

_[8] K. N. Plunkett, K. L. Berkowski, J. S. Moore, *Biomacromolecules* **2005**, *6*, 632.

_[9] S. Kim, K. E. Healy, *Biomacromolecules* **2003**, *4*, 1214.

_[10] S. G. Lévesque, M. S. Shoichet, *Bioconjugate Chem.* **2007**, *18*, 874.

_[11] B. D. Mather, S. R. Williams, T. E. Long, *Macromol. Chem. Phys.* **2007**, *208*, 1949.

_[12] Kafouris, E. Themistou, C. S. Patrickios, *Chem. Mater.* **2006**, *18*, 85.

_[13] B. G. Stubbe, F. Horkay, B. Amsden, W. E. Hennink, S. C. de Smedt, J. Demester, *Biomacromolecules*, **2003**, *4*, 691.

_[14] N. Murthy, M. Xu, S. Schuck, J. Kunisawa, N. Shastri, J. M. J. Fréchet, *Proc. Natl. Acad. Sci. USA* **2003**, *100*, 4995.

_[15] E. M. Bachelder, T. T. Baudette, K. E. Broaders, S. E. Paramanov, J. Dashe, J. M. J. Fréchet, *Mol. Pharmaceutics* **2008**, *15*, 876.

_[16] D. K. Sahanna, G. Mittal, V. Bhardwaj, M. N. V. Ravi Kumar, *J. Pharm. Sci.* **2008**, *97*, 1530.

_[17] A. Musyanovych, J. Schmitz-Wienke, V. Mailander, P. Walther, K. Landfester, *Macromol. Biosci.* **2008**, *8*, 127.

_[18] S. Bauhuber, C. Hozsa, M. Breunig, A. Göpferich, *Adv. Mater.*, **2009**, *21*, 3286.

_[19] T. Söderdahl, M. Enoksson, M. Lundberg, A. Holmgren, O. P. Ottersen, S. Orrenius, G. Bolcsfoldi, I. A. Cotgreave, *FASEB J.* **2002**, *16*, 124.

_[20] J. K. Oh, D. J. Siegwart, K. Matyjaszewski, *Biomacromolecules* **2007**, *8*, 3326.

_[21] J. K. Oh, D. J. Siegwart, H. Lee, G. Sherwood, L. Peteanu, J. O. Hollinger, K. Kataoka, K. Matyjaszewski, *J. Am. Chem. Soc.* **2007**, *129*, 5939.

_[22] R. K. Kainthan, S. R. Hester, E. Levin, D. V. Devine, D. E. Brooks, *Biomaterials* **2007**, *28*, 4581.

_[23] C. Siegers, M. Biesalski and R. Haag ,*Chem. Eur. J.*, **2004**, *10*, 2831 – 2838.

_[24] R. Tokar, P. Kubisa and S. Penczek, *Macromolecules* **1994**, *27*, 320.

_[25] A. Dworak, W. Walach, B. Trzebicka, *Macromol. Chem. Phys.* **1995**, *196*, 1963.

_[26] E. J. Vandenberg, *J. Polym. Sci. Polym. Chem. Ed.* **1985**, *23*, 915.

_[27] A. Sunder, R. Hanselmann, H. Frey, R. Mülhaupt, *Macromolecules* **1999**, *32*, 4240.

_[28] M. Calderon, M. A. Quadir, S. K. Sharma, R. Haag, *Adv. Mater.* **DOI:** 10.1002/adma.200902144

_[29] S. Xu, Y. Luo, R. Graeser, A. Warnecke, F. Kratz, P. Hauff, K. Licha, R. Haag, *Biorg. Med. Chem. Lett.* **2009**, *19*, 1030.

_[30] M. Krämer, J. -F. Stumbé, H. Türk, S. Krause, A. Komp, L. Delineau, S. Prokhorova, H. Kautz, R. Haag, *Angew. Chem. Int. Ed.* **2002**, *41*, 4252.

_[31] R. K. Kainthan, E. B. Muliawan, S. G. Hatzikiriakos, D. E. Brooks, *Macromolecules* **2006**, *39*, 7708.

_[32] S. Zhang, J. Li, G. Lykotrafitis, G. Bao, S. Suresh, *Adv. Mater.* **2009**, *21*, 419.

_[33] A. L. Sisson, D. Steinhilber, T. Rossow, P. Welker, K. Licha, R. Haag, *Angew. Chem. Int. Ed.* **2009**, *48*, 7540 - 7545.

_[34] K. Landfester, *Angew. Chem. Int. Ed.* **2009**, *48*, 4488.

_[35] The precise batch of surfactant used is a poly(ethylene-co-butylene)-block-poly(ethylene oxide), Mn 8,100, 41 wt.% ethylene oxide, 39 wt. % ethylene, 20 wt. % butylene as used in; J. K. Oh, H. Dong, R. Zhang, K. Matyjaszewski, H. Schlaad, *J. Polym. Sci. Part A: Polym. Chem.*, **2007**, *45*, 4764: Synthetic details given in; A. Thomas, H. Schlaad, B. Smarsly, M. Antonietti, *Langmuir*, **2003**, *19*, 4455.

_[36] T. Tadros, P. Izqierdo. J. Esquena, C. Solans, *Adv. Colloid Interface Sci.* **2004**, *108 - 109*, 303.

_[37] S. Gronowitz, B. Herslof, P. Michelsen, B. Akkeson, *Chem. Phys. Lipids* **1978**, *22*, 307.

_[38] Was prepared from the parent diol following established synthetic protocol: H-C. Kang, B. M. Lee, J. Yoon, M. Yoon, *J. Am. Oil Chem. Soc.* **2001**, *4*, 424.

_[39] A. L. Sisson, I. Papp, K. Landfester, R. Haag, *Macromolecules*, **2009**, *42*, 556.

_[40] A. N. Zelikin, J. F. Quinn, F. Caruso, *Biomacromolecules* **2006**, *7*, 27.

_[41] A. N. de Belder, K. Granath, *Carbohydr. Res.* **1973**, *30*, 375.

_[42] H. Türk, S. Mecking. R. Haag. German patent application DE 10211664A1, **2003**.

_[43] R. Haag, F. Kratz, *Angew. Chem. Int. Ed.* **2006**, *45*, 1198.

_[44] P. Caliceti, F. M. Veronese, *Adv. Drug Del. Rev.* **2003**, *55*, 1261.

_[45] Note on terminology: Here the symbol "•" denotes supramolecular/physical complex, e.g. **5g•IDCC** means IDCC dye complexed nanogels **5g**.

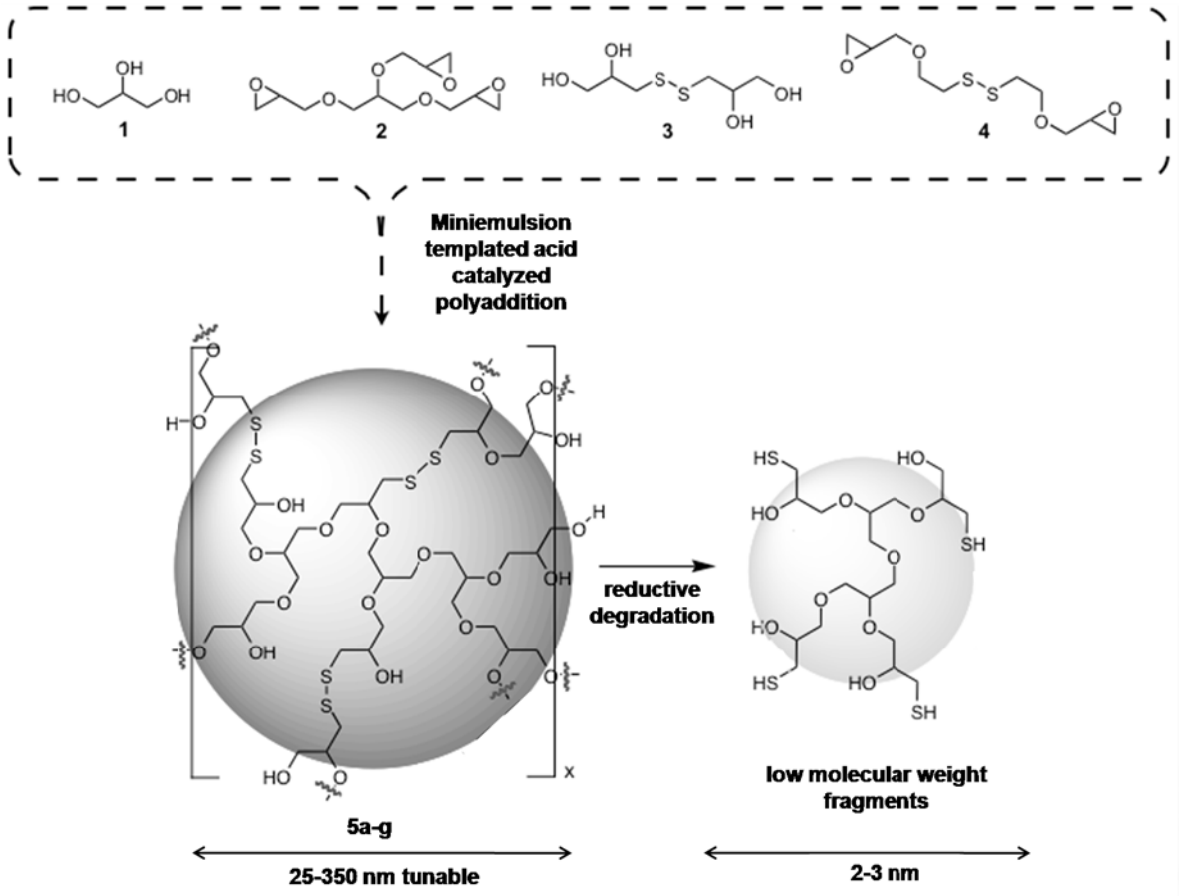

Scheme 1. Synthetic route to biodegradable polyglycerol nanogels, showing a generalized structure depiction of nanogel and degradation fragment.

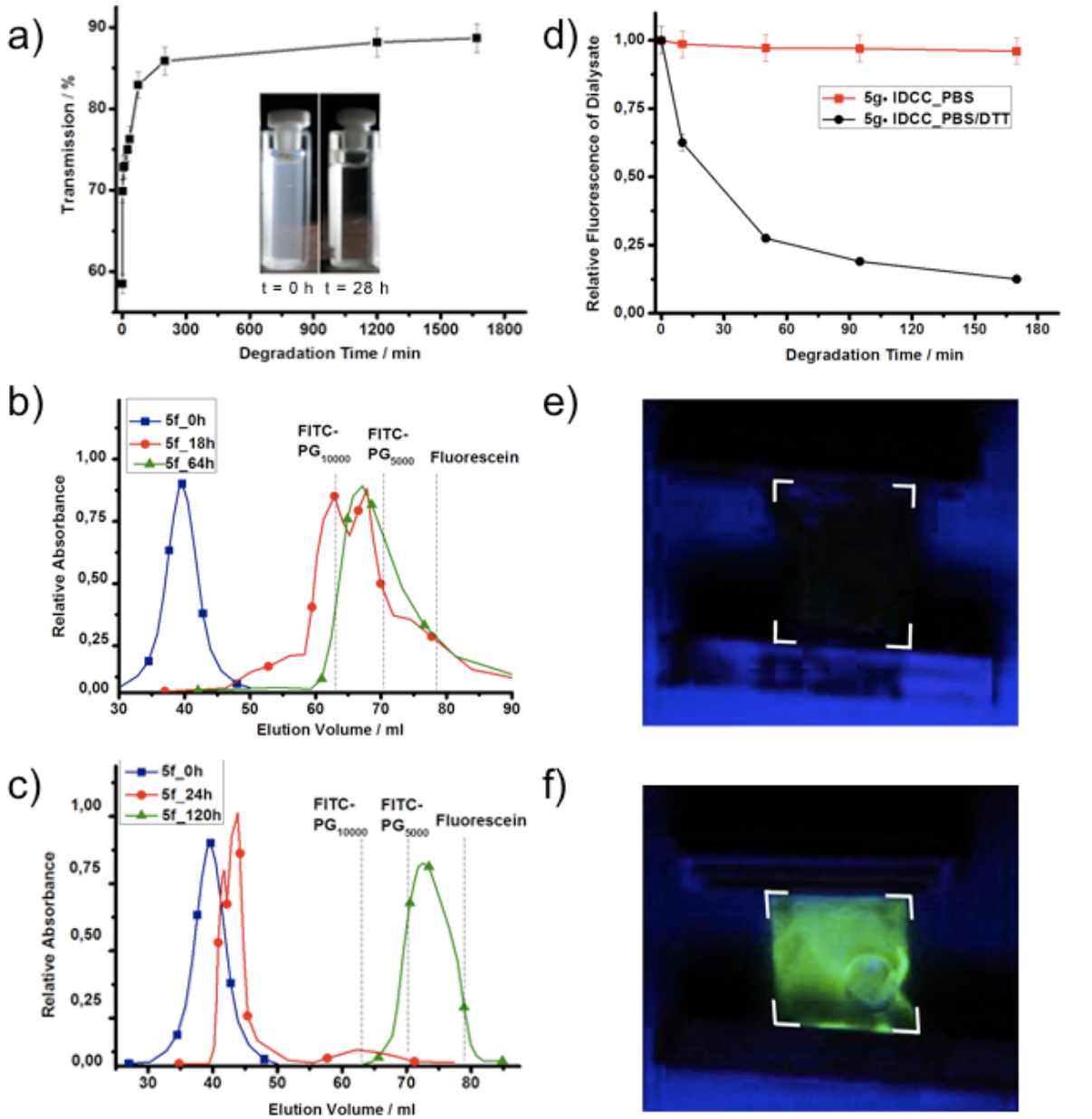

Figure 1. a) UV-vis transmission at λ = 700 nm of sample **5d** at time intervals after addition of reducing agent, and inset: Dispersions at time 0 min. (left) and 1,670 min. (right); b), c) GPC traces of **5f-FITC** degradation at varying times using as reducing agent DTT (b) and glutathione c). Average retention times of known hyperbranched polyglycerol standards (5,000 and 10,000 Dalton average molecular weight), and fluorescein are depicted as reference; d) Time dependent IDCC fluorophore leakage from dialysis tubing measured by fluorescence spectroscopy after degradation of the dye loaded nanogel **5g•IDCC**; e), f) Visual observation of the complete release of fluorescein after 2 d from dye loaded nanogels **5g•Fl** after dialysis in DTT containing buffer e), and in the absence of reducing agents f).

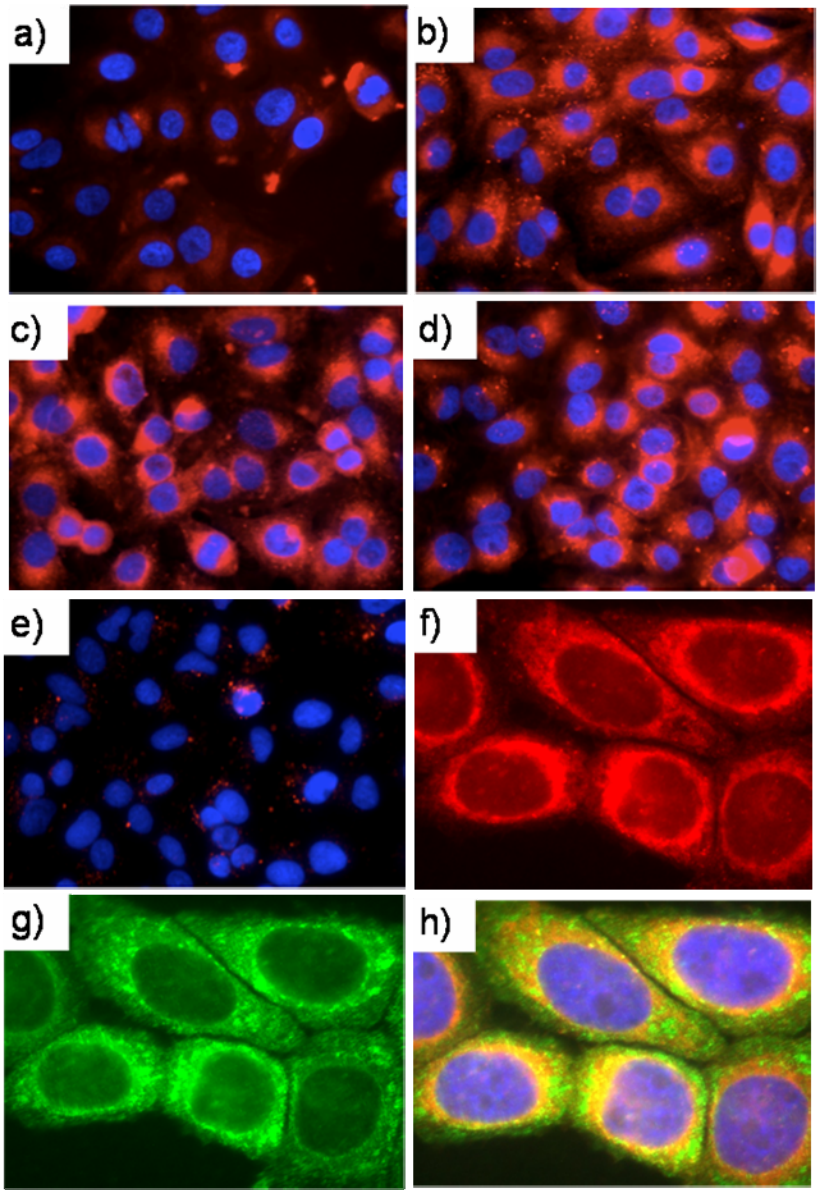

Figure 2. a) – d) Optical microscope image of the human lung cancer cell line A549 incubated at 37 °C with **5g-RITC** (red) for a) 0.5 h, b) 1 h., c) 4 h, d) 24 h, and, e) incubated in the presence of low molecular weight control (glycerol-RITC) for 24 h at 37 °C. Nuclei were stained with 4',6-diamidino-2-phenylindole (DAPI, blue), f) - h) Culture of human cervix carcinoma cells (CASKI) at 37 °C with **5g-RITC** for 1h - f). Endosomes were stained with anti-Mannose-6-phosphate-receptor (late endosome marker) g). In case of co-localization of vesicle (green) and **5g-RITC** (red) a yellow colour can be observed h). Nuclei were stained with DAPI (blue).

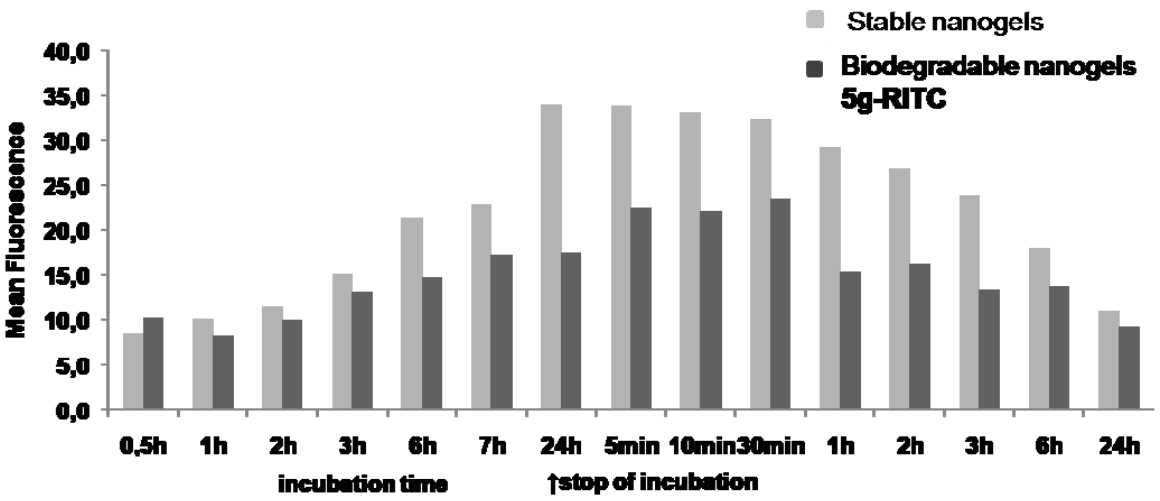

Figure 3. Flow cytometric analysis of human lung cancer cells A549 incubated with stable polyglycerol nanogels (grey) and biodegradable nanogels **5g-RITC** (black) incubated with nanogel medium (left) or normal culture medium (right). Fluorescence was detected at 570 nm.

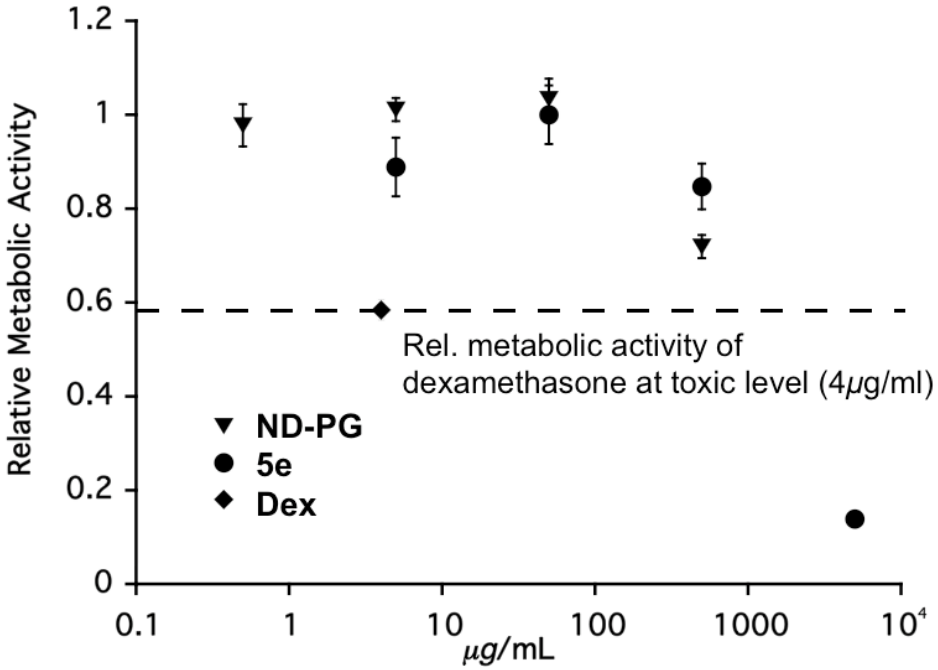

Figure 4. Relative metabolic activity tests (MTT, human hematopoietic U-937 culture) of nanogel **5e**, compared on a w/w basis to dexamethasone (DEX) and non-degradable polyglycerol nanogels (ND-PG; as in reference [33]). Metabolic activity is shown relative to control activity in the absence of analytes (buffer only).

Table 1. Varying the monomer content prior to miniemulsion leads to nanogels with different characteristics (solubility, size, incidence of degradable units)

	Proportion (mg)						
Product	**1**	**2**	**3**	**4**	DMSO (ml) [b]	Diameter (nm) [a]	Solubility
5a		170	100		0.05	340 ± 41	dispersed
5b		170	100		0.1	308 ± 28	dispersed
5c		170	100		0.3	124 ± 11	dispersed
5d		170	100		0.5	91 ± 5	dispersed
5e	62	213	87		0.5	62 ± 10	dissolved
5f	38	222	141		0.5	56 ± 11	dissolved
5g	147			349	0.1	23 ± 5	dissolved

[a] Constant parameters: cyclohexane (15 ml); surfactant (20 mg). [b] Average, measured by dynamic light scattering.

Submitted to ADVANCED FUNCTIONAL MATERIALS

Biodegradable, functional nanoparticles based on size-defined, disulfide-linked polyglycerol nanogels are a new class of cellular delivery vehicles. Their preparation via miniemulsion polymerization is simple, versatile, and controllable to fine tune material properties. By various methods we reveal how these hydrophilic materials degrade into small fragments in reducing environments. We demonstrate that these materials show little toxicity and rapidly endocytose into cells.

Keyword: Stimuli-Responsive Materials

D. Steinhilber, A. L. Sisson, D. Mangoldt, P. Welker, K. Licha, R. Haag*

Synthesis, Reductive Cleavage and Cellular Interaction Studies of Biodegradable, Polyglycerol Nanogels

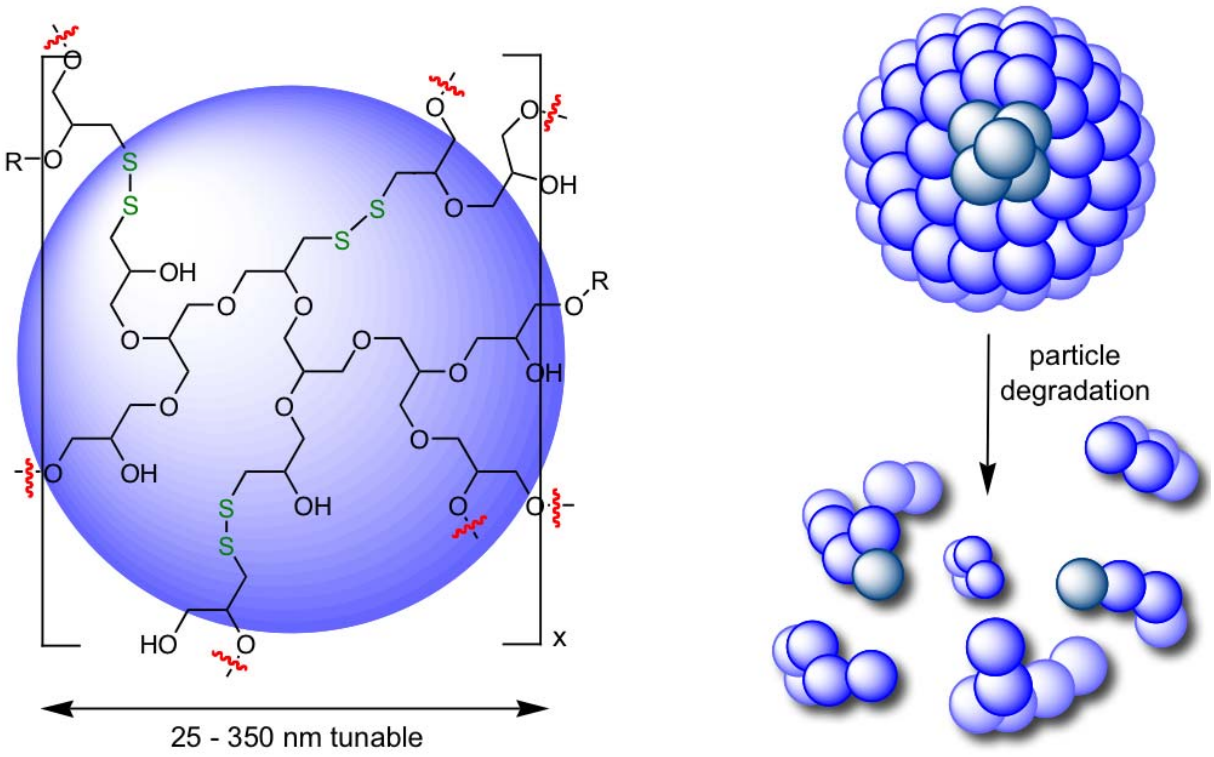

Submitted to ADVANCED FUNCTIONAL MATERIALS

Supporting information

Synthesis, Reductive Cleavage and Cellular Interaction Studies of Biodegradable, Polyglycerol Nanogels

By *Dirk Steinhilber, Adam L. Sisson*, *Dorothea Mangoldt, Pia Welker, Kai Licha,* and *Rainer Haag**

Dedicated to Professor George Whitesides on the occasion of his 70th birthday

[*] Prof. R. Haag, D. Steinhilber
Institute for Chemistry and Biochemistry
Free University Berlin
Takustrasse 3, Berlin 14195 (Germany)
E-mail: haag@chemie.fu-berlin.de
Dr. A. L. Sisson
GKSS Forschungszentrum Geesthacht
Institute for Polymer Research
Kantstrasse 55, Teltow-Seehof 14513 (Germany)
Dr. P. Welker, Dr. K. Licha
mivenion GmbH
Robert-Koch-Platz 4, Berlin 10115 (Germany)

Synthetic Procedures

Preparation of FITC-labelled nanogels ***5f-FITC*** *and FITC-labelled hyperbranched polyglycerols (hPG)(M_W =5 kDa, 10 kDa)*

FITC labelled nanogels and hPGs [1] were prepared following the literature procedure [2]. Either nanogel **5f** or hPGs *(M_W = 5 kDa, 10 kDa)* (10 mg) and FITC (1 mg, 0.026 mmol) were dissolved in dry DMSO (1 ml). After addition of dibutyltin dilaurate catalyst (10 µl), the reaction mixture was heated at 90 °C for 2 h. The product was purified from free FITC by intensive dialysis in ethanol (5 d, 3 times solvent exchange per day).

Preparation of RITC-labelled nanogels ***5g-RITC*** *and RITC-labelled hyperbranched polyglycerols (hPG)(M_W =5 kDa, 10 kDa)*

RITC labelled nanogels and hPGs [1] were prepared following the literature procedure [2]. Either nanogel **5g** and hPGs *(M_W = 5 kDa, 10 kDa)* (10 mg) and RITC (1 mg, 0.026 mmol) were dissolved in dry DMSO (1ml). After addition of dibutyltin dilaurate catalyst (10 µl), the reaction mixture was heated at 90 °C for 2 h. The product was purified from free RITC by intensive dialysis in ethanol (5 d, 3 times solvent exchange per day).

Encapsulation of Indocarbodicyanine dye (IDCC) and Fluorescein

The same synthetic procedure, as described for the nanogel preparation **5a**-**5g,** was applied, however this time IDCC dye (previously reported in [3]) (1 mg) or Fluorescein (1 mg) was dissolved in the dispersed phase (monomers/DMSO) prior to miniemulsification.

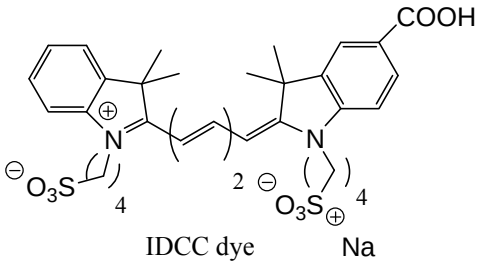

*Synthesis of Hydroxyethyldisulfide-bis-glycidylether **4***

The monomer was prepared from the parent diol following an established synthetic protocol [4]. Briefly, to a 50 ml three necked flask 2-hydroxyethyl disulfide (0.39 ml, 2.87 mmol), sodium hydroxide (395.4 mg, 9.78 mmol) and tetrabutylammonium bromide (TBAB) (7.1 mg, 0.02 mmol) were added and heated to 40 °C. Epichlorohydrin (0.83 ml, 10.59 mmol) was added slowly over a dropping funnel and the reaction was stirred for 3 h. The product was purified by column chromatography (n-hexane/ethyl acetate, 1:4) to obtain the dithio-derivative **4** as a yellow liquid (105 mg, 20%).

^{1}H NMR (CD_3Cl, 250 MHz, 25 °C, TMS, δ): 3.80-3.66 (m, 6H), 3.40-3.33 (m, 2H), 3.15-3.09 (m, 2H), 2.89-2.84 (t, 4H), 2.79-2.75 (m, 2H), 2.60-2.57 (m, 2H).

^{13}C NMR (CD_3Cl, 250 MHz, 25 °C, TMS, δ): 71.72, 69.62, 50.79, 44.12, 38.57; MS (m/z): 265.9 $[M+H]^+$.

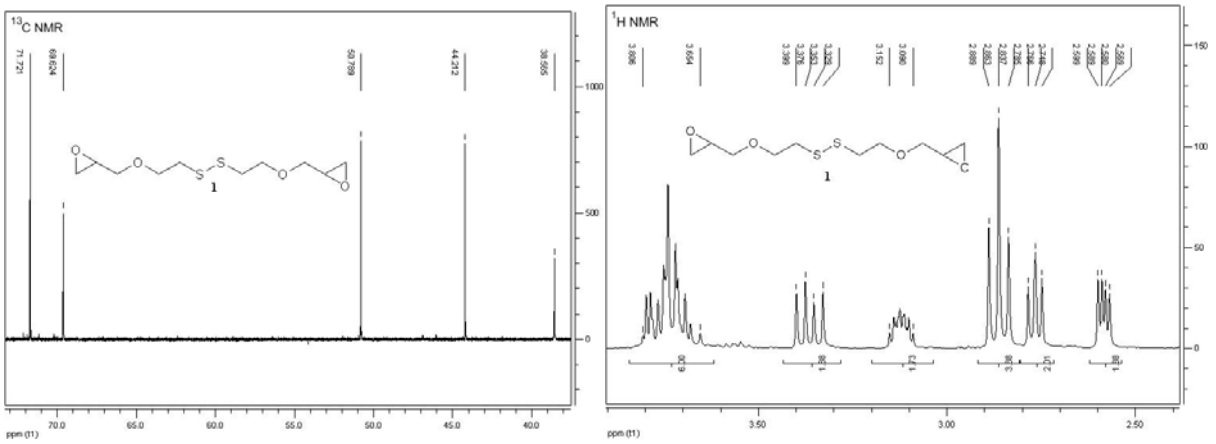

Fig. S1. ^{1}H NMR (250 MHz, $CDCl_3$, 25°C), ^{13}C NMR (80 MHz, $CDCl_3$, 25°C) of monomer **4**.

Nanogel Characterization

Dynamic Light Scattering (DLS)

DLS histograms (left) and correlation functions (right) for product **5a**

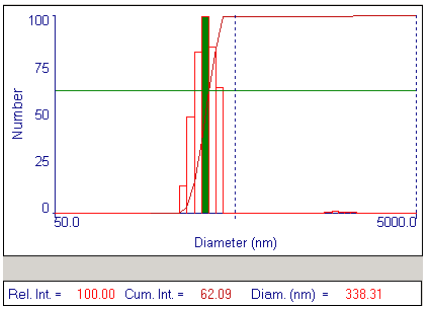

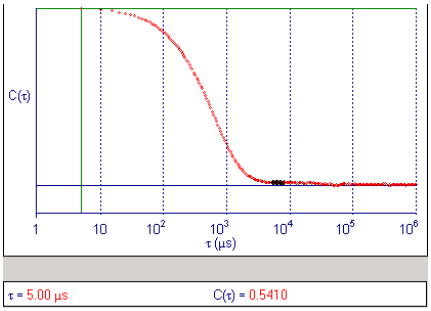

DLS data for product **5b**

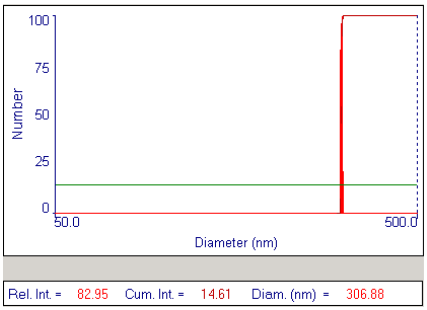

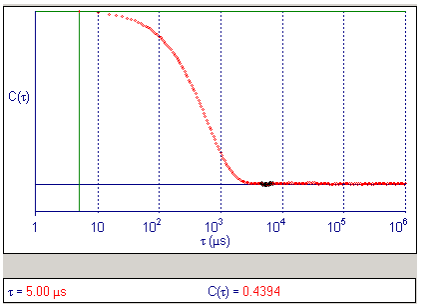

DLS data for product **5c**

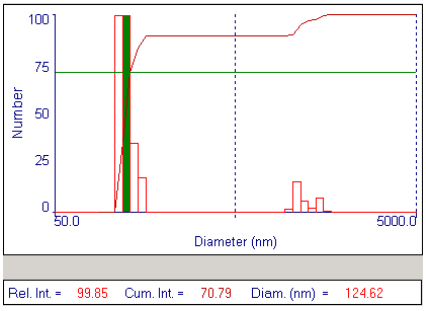

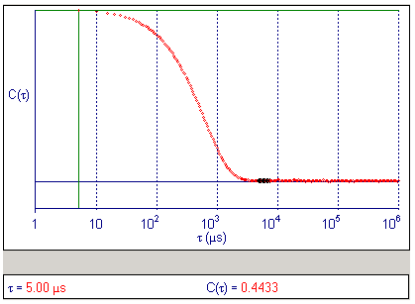

DLS data for product **5d**

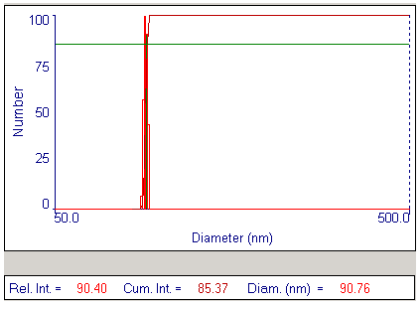

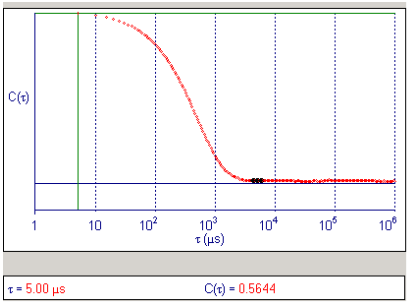

Fig. S2a. DLS histograms (left) and correlation functions (right) for products **5a-5d**.

DLS data for product **5e**

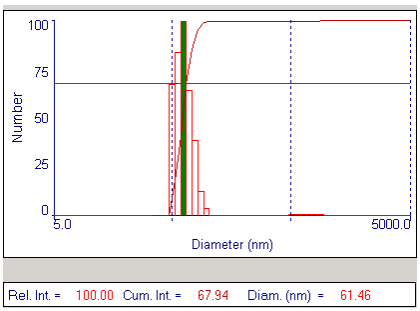

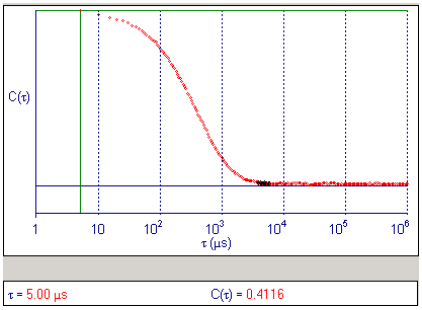

DLS data for product **5f**

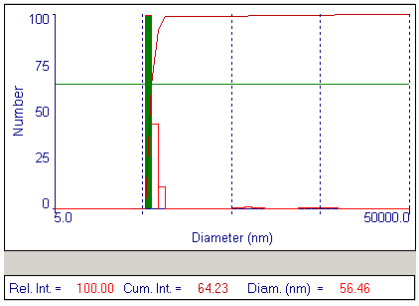

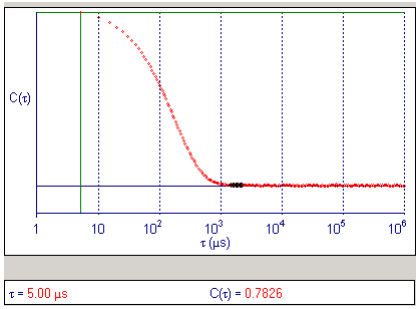

DLS data for product **5g**

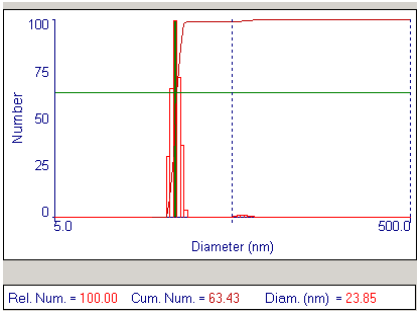

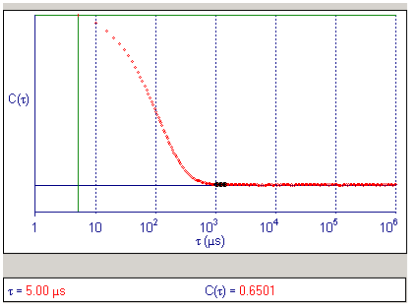

DLS data for product **5g-RITC**

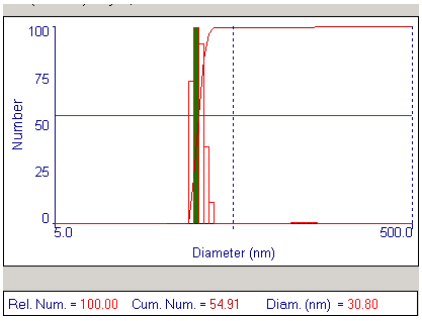

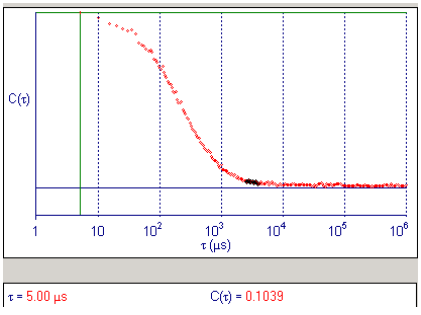

Fig. S2b. DLS histograms (left) and correlation functions (right) for products **5e-5g-RITC.**

DLS data for stable, RITC-labelled polyglycerol nanogel

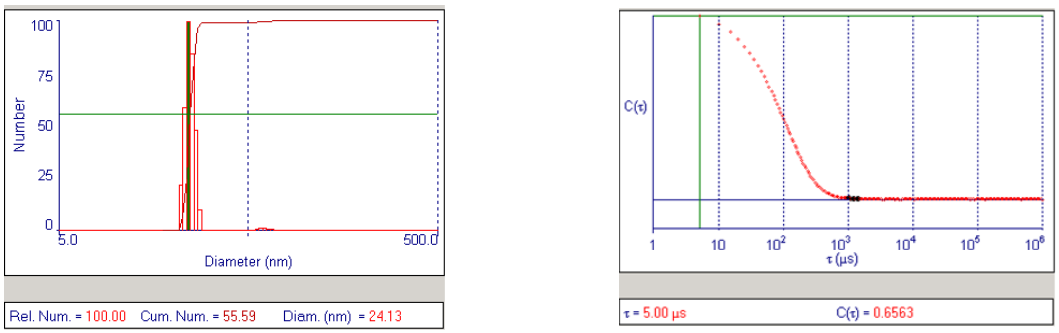

Fig. S2c. DLS histograms (left) and correlation functions (right) for RITC-functionalized stable polyglycerol nanogel**.**

Nanogel degradation

UV-vis turbidity measurement

Disulfide containing nanogel (10 mg, **5d**) was dispersed in PBS-buffer (pH 7.4, 3 ml) and filled into a UV-vis cuvette, equipped with a magnetic stirrer. After recording the transmission spectrum of the pure nanogel solution, the sample was degassed, DTT (10 mg, 0.065 mmol) was added and the cuvette was sealed airproof. Finally, transmission spectra were recorded in certain time intervals (Figure 1a). In between the measurements, the sample was magnetically stirred.

[1]H-NMR-spectroscopy

Nanogel **5d** (20 mg) was dissolved in (CD_3OD (0.5 ml) and a ^{1}H-NMR spectrum was recorded (upper spectrum). After addition of triphenylphosphine the solution was stirred over night at room temperature and another ^{1}H NMR spectrum was recorded (lower spectrum).

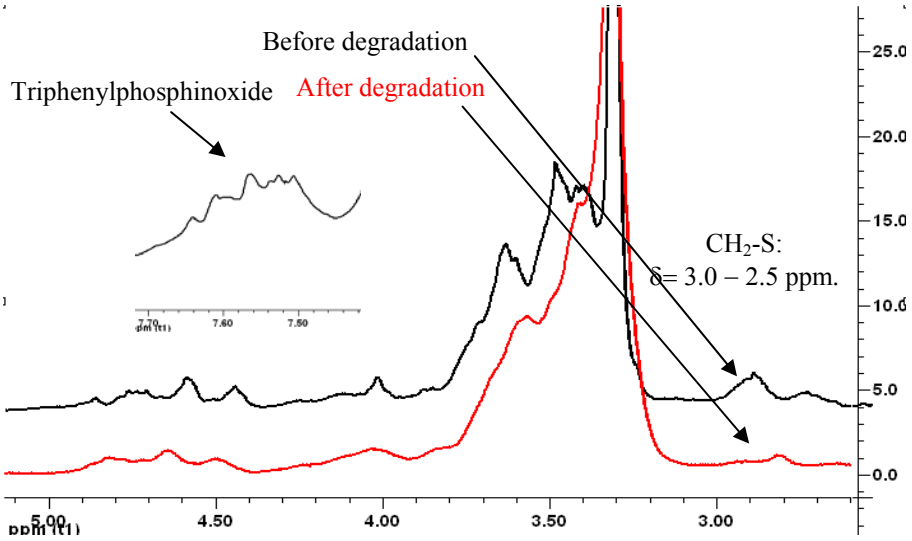

Fig. S3. ^{1}H-NMR spectrum of nanogel **5d** before addition of triphenyl-phosphine (upper spectrum); ^{1}H-NMR spectrum of degraded nanogel after addition of triphenylphosphine (lower spectrum) in CD_3OD.

Size exclusion chromatography

Size Exclusion Chromatography (SEC) measurements were performed on PSS Suprema columns (serious connection of 100 Å, 100-100000 Da; 1000 Å, 100-1000000 Da; and 3000 Å, 100-3000000 Da) in Phosphate Buffered Saline (pH 7.4) as eluent, UV-vis detector set on 450 nm, flow rate 1 ml/min. Briefly, solutions of FITC labelled nanogels **5f** and RITC labelled nanogels **5g** in PBS buffer (50 µg/ml, pH 7.4) were prepared and chromatograms of the nanogels were taken. After degassing the solutions for 30 min, they were incubated with DTT (50 mM, r.T.) and glutathione (5 mM, 37 °C) under magnetic stirring and the samples were injected into the GPC column (Figure 1b), 1c) and figure below).

Interestingly, we observed that incubation of **5g-RITC** with glutathione (5 mM, 37 °C, see figure below) resulted in much longer retention times and lower molecular weights of the degraded fragments, compared to **5f-FITC.** The lower molecular weights can be explained by the increased amount of disulfide crosslinks in **5g-RITC.**

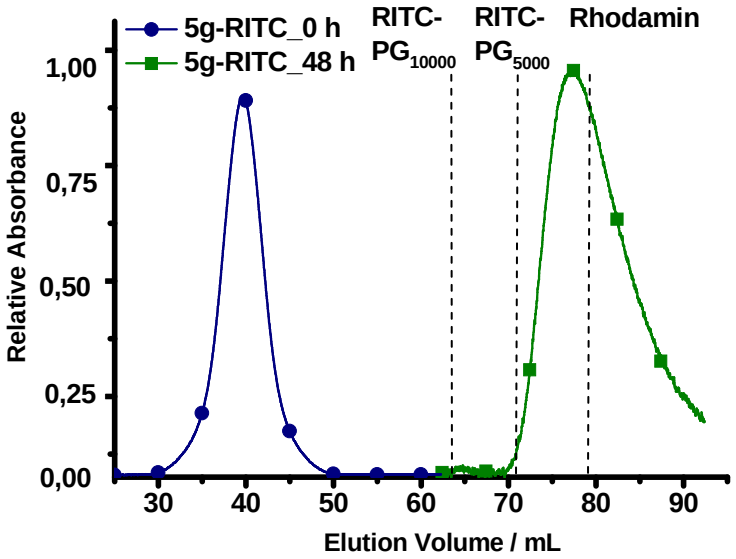

Fig. S4. GPC traces of **5g-RITC** degradation after 0 h (blue) and 48 h (green) times using glutathione as reducing agent.

Dialysis

Degradation of nanogels **5g•IDCC** and **5g•Fl** was studied by dye release from a dialysis tube. Two solutions of nanogels (10 mg) in PBS buffer (10 ml, pH 7.4) were filled into dialyis tubes. One tube was dialysed against pure PBS buffer (pH 7.4) and the other tube was dialysed in a reductive environment (50 mM DTT solution in PBS). At the time intervals shown in the graph below, samples were taken from the dialysis tubes and fluorescence spectra were taken (excitation wavelength: 600 nm). The decrease in fluorescence intensity from samples dialysed in pure PBS buffer was attributed to dye leaching from the nanogels, which was not triggered by degradation. The fluorescence dyes were not affected in the reducing environment (fluorescence did not decrease over time). Additionally, nanogels **5g•IDCC** and **5g•Fl** were stable in PBS buffer for several weeks (SEC). The decrease in fluorescence within the dialysis tubes in the reductive environment (Figure 1d)-1f) and Figure below) can be exclusively attributed to reductive degradation of the nanogels into smaller fragments with concomitant release of the entrapped dye.

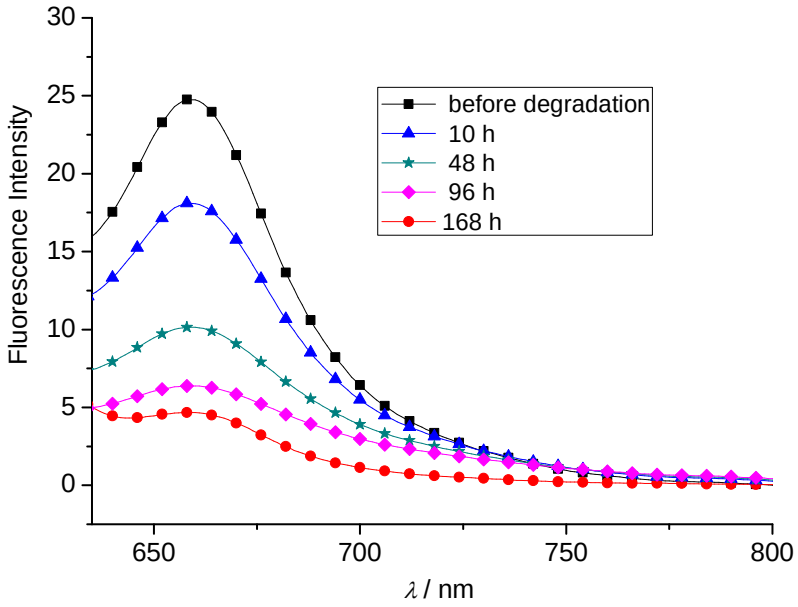

Fig. S5. Decrease in fluorescence (within dialysis tube) over time as dye labelled nanogels (**5g•IDCC**) were degraded and then released from dialysis tubing.

Cell Studies

*Cellular uptake of **5g-RITC** into cell line A549 (Figure 2a)-e))*

The epithelial human lung cancer cell line A549 was routinely propagated as follows: DEMEM medium, with 10% fetal calf serum (FCS), 2% glutamine, and penicillin/streptomycin (all from PAN Biotech) was added. Cells were seeded into medium at $1 \cdot 10^5$ cells/ml, cultured at 37 °C with 5% CO_2, and split 1:5 two times a week.

Histochemical staining: In the present study, cells were seeded at $2 \cdot 10^5$ cells/ml in a 24-well culture plate on glass coverslips (Sigma), and cultured for 24 h at 37 °C. Thereafter, cells were cultured with medium containing $1 \cdot 10^{-7}$ M **5g-RITC** or $1 \cdot 10^{-5}$ M **glycerol-RITC** for 4 h at 37 °C. Molarity was adjusted based on the assumption of a 5 Million molecular weight. Afterwards, cells were fixed with cold acetone and 4,6-diamidino-2-phenylindole (DAPI, Abcam) was used for nuclear counterstain. Image acquisition was performed using a Leica DMRB microscope (Leica). Images were taken with a digital camera (Spot 32, Diagnostic Instruments).

*Cellular uptake of **5g-RITC** into human hematopoietic celline U937 (see figures below)*

The human hematopoietic cellline U937 was routinely propagated as follows: RPMI medium, with 10% fetal calf serum (FCS) and penicillin/streptomycin (all from PANBiotech) was

added. Cells were seeded into medium at $1 \cdot 10^5$ cells/ml, cultured at 37 °C with 5 % CO_2, and split 1:30 two times a week.

In the present study, non-adherent U937 cells were seeded at $5 \cdot 10^5$ cells/ml in a 24-well culture plate on glass coverslips (Sigma) and cultured for 24 h at 37 °C with 10 ng/ml phobolmyristate acetate (differentiation of cells towards macrophages). Thereafter, the living cells were cultured with medium containing $1 \cdot 10^{-5}$ M **glycerol-RITC** (negative control) or product **5g-RITC** for 30 min, 1, 4, or 24 h at 37 °C. Afterwards, cells were fixed with cold PFA (the cells were not able to actively transport any more now), rinsed, and covered with 4,6-diamidino-2-phenylindole (DAPI, Abcam) for nuclear counterstain. Image acquisition was performed using a Leica DMRB microscope. All images were taken with the same exposure time of 2000 ms in order to compare the fluorescence signal intensities.

The uptake started in the first 30 min of incubation and increased up to 24 h. The culture with **5g-RITC** for 24 or 48 h generated points of highly colored fluorescence signals, which could be endocytotic vesicles. These vesicles are clearly demonstrated in U937 cells differentiated in macrophages with PMA, and cultured with **5g-RITC** for 4 h (B and C).

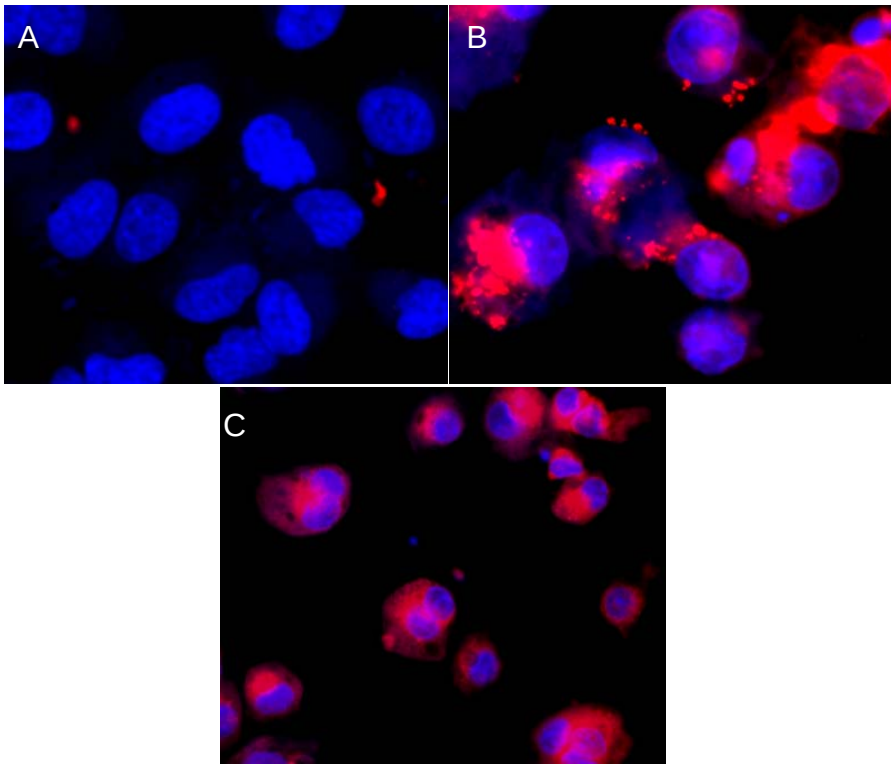

Fig. S6. Culture of the human hematopoetic cell line U937 stimulated with PMA with **glycerol-RITC** as negative control (A) or **5g-RITC** (red) (B, C) for 4 h at 37 °C. Nuclear staining with DAPI (blue). Magnification 650x (A, B) or 250 (C).

*Cellular uptake of **5g-RITC** into epithelial human cancer cell line CASKI with late endosomal staining (Figure 2f)-h))*

The epithelial human cancer cell line CASKI was routinely propagated as follows: DEMEM medium, with 10 % fetal calf serum, 2 % glutamine, and penicillin/streptomycin (all from PAN Biotech) was added. Cells were seeded into medium at $1 \cdot 10^5$ cells/ml, cultured at 37 °C with 5 % CO_2, and split 1:5 two times a week.

Cytochemistry: Cells were seeded at $5 \cdot 10^4$ cells/ml in a 24-well culture plate on glass coverslips (Sigma), and cultured for 24 h at 37 °C. Thereafter, cells were cultured with medium containing $1 \cdot 10^{-6}$ M of **5g-RITC** or $1 \cdot 10^{-6}$ M **glycerol-RITC** as negative control. Afterwards, cells were fixed with cold acetone, rinsed, and incubated for 1 h in a dilution of 1,300 with a rabbit polyclonal anti-mannose-6-phosphate-receptor antibody (Abcam) and a Cy-2-labeled anti rabbit secondary antibody (Dianova). 4,6-diamidino-2-phenylindole (DAPI, Abcam) was used for nuclear counterstain. Image acquisition was performed using a Leica DMRB microscope (Leica). Images were taken with a digital camera (Spot 32, Diagnostic Instruments).

Uptake kinetics studied by fluorescence activated cell sorting (FACS, figure 3)

$2 \cdot 10^5$ cells/ml A549 cells were cultured in 24-well-plates with normal culture medium or medium containing $1 \cdot 10^{-8}$ M test substances **5g-RITC** and stable polyglycerol nanogels for different time periods. Thereafter, cells were washed with PBS and detached with 200 µl/well accutase (PAA) and washed two times with PBS. Cells were fixed with 500 µl 3% paraformaldehyde for 10 min at 4 °C, stopped with 2 ml PBS and centrifuged with 250 g, for 10 min at 4 °C. Supernatants were removed and cells were suspended in 200 µl PBS with 0.5% bovine serum albumin (Roth). Fixed cells were kept at 4 °C until they were analysed in a FACS Calibur analysis instrument (Becton-Dickinson). Mean fluorescence of all cells at 570 nm was detected and the difference to the mean fluorescence of control substance (glycerol-ICC) was calculated (Diff. mean fluor. 570 nm).

Glutathione inhibition (study as similarly described in [5])

For the glutathione inhibition study $2 \cdot 10^5$ cells/ml A549 cells were precultured in 24-well plates with a 10 µm N-ethylmaleimide medium or with normal culture medium, following the culture with medium containing $2 \cdot 10^{-6}$ M test substances **5g-RITC** and stable polyglycerol nanogels. After 24 h the cells were cultured again with 10 µm N-ethylmaleimide medium or

with normal culture medium. Thereafter, cells were washed with PBS and detached with 200 µl/well accutase (PAA) and washed two times with PBS. Cells were fixed with 500 µl 3% paraformaldehyde for 10 min at 4 °C, stopped with 2 ml PBS and centrifuged with 250 g, for 10 min at 4 °C. Supernatants were removed and cells were suspended in 200 µl PBS with 0.5% bovine serum albumin (Roth). Fixed cells were kept at 4 °C until they were analysed in a FACS Calibur analysis instrument (Becton-Dickinson). Mean fluorescence of all cells at 570 nm was detected and the difference to the mean fluorescence of control substance (glycerol-ICC) was calculated (Diff. mean fluor. 570 nm).

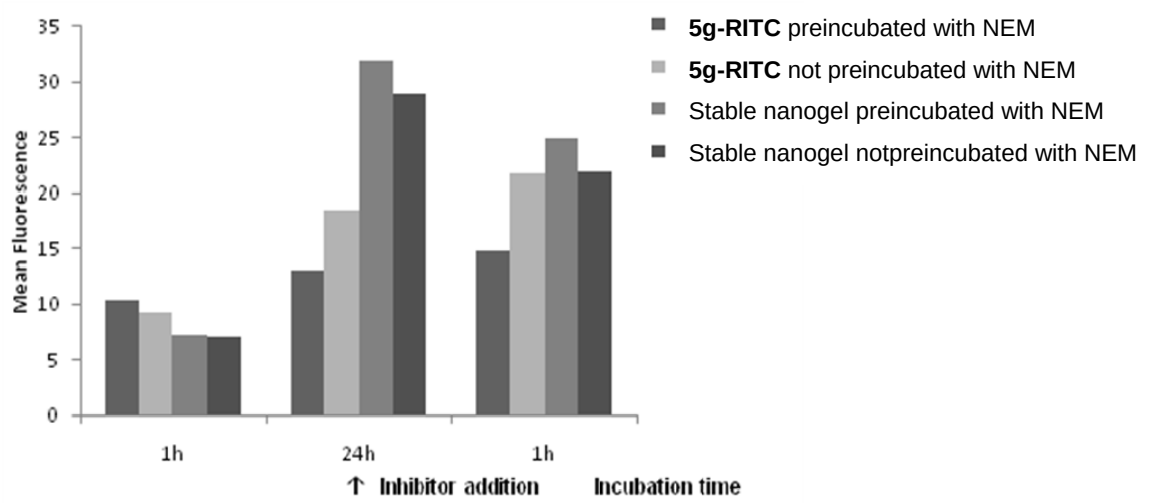

Fig. S7. Flow cytometric analysis of human lung cancer cells A549 incubated for different times with culture medium with and without addition of glutathione inhibitor N-ethylmaleimide, containing nanogels **5g-RITC** or stable polyglycerol nanogel.

In order to prove, that the reduced cellular fluorescence intensity of **5g-RITC** compared to the stable nanogel (figure 4) is due to intracellular reduction of the disulfide bonds, we performed FACS analyses on human lung cancer cells A549 with and without glutathione inhibitor N-ethylmaleimide [5]. It is interesting to note that nanogels **5g-RITC** showed again lower fluorescence intensities in the intracellular reducing environment (without inhibitor) as compared to the inhibited reducing environment (with inhibitor).

Cytotoxicity assays

These analyses were performed with cells cultured in 24 well plates. $2 \cdot 10^5$ cells/ml were incubated in 1 ml culture medium containing an increasing concentration of test substance **5e**. Incubation of cells with $1 \cdot 10^{-5}$ M dexamethasone (Sigma) was used as a positive control for induction of apoptosis. After 2 d of culture, cell number and viability were analyzed in a cell counter and analyzer system (CASY®, Schärfe Systems). Experiments were done at least in quadruplicate. In addition, drug cytotoxicity was assessed in vitro using the MTT assay (cellular reduction of 3-(4,5-dimethylthiazol-2-yl)-2,5-diphenyltetrazolium bromide) as a test for metabolic activity of the cells. Briefly, $1 \cdot 10^4$ cells per well were plated in 96-well plates in 100 µl culture medium containing an increasing concentration of the test substance. After 2 d of culture, 10 µl MTT (5 mg/ml in PBS, obtained from Sigma) was added to each well and the plates were incubated for 4 h. The resulting formazan product was dissolved with acid isopropanol and the absorbance at a wavelength of 570 nm (Ex570) was read on a Microplate Spectrophotometer (Anthos htII, Microsystems).

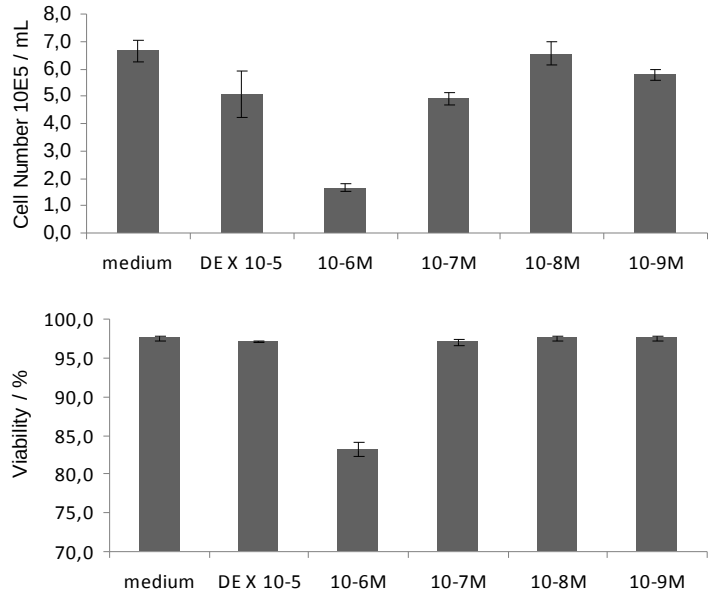

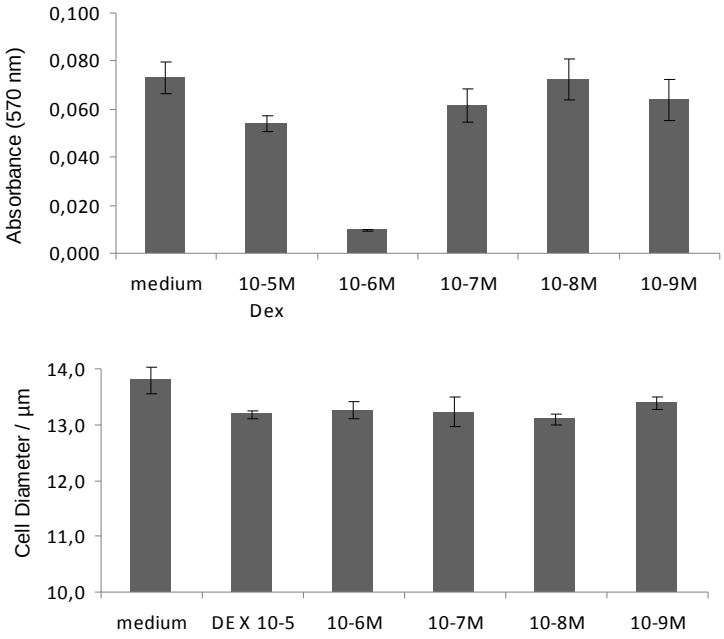

Fig. S8. Human hematopoietic U-937 cell proliferation (cell number), viability, and metabolic activity (MTT) tests on nanogel **5e** with negative and positive controls.

References

_[1] H. Türk, S. Mecking. R. Haag. German patent application DE 10211664A1, **2003**

_[2] A. N. de Belder, K. Granath, *Carbohydr. Res.* **1973**, *30*, 375.

_[3] K. Licha, C. Hessenius, A. Becker, P. Henklein, M. Bauer, S. Wisniewski, B. Wiedenmann, W. Semmler, *Bioconjugate Chem.* **2001**, *12*, 44.

_[4] H-C. Kang, B. M. Lee, J. Yoon, M. Yoon, *J. Am. Oil Chem. Soc.* **2001**, *4*, 424.

_[5] J. Yang, H. Chen, I. R. Vlahov, J.-X. Cheng, P. S. Low, *Proc. Natl. Acad. Sci. U. S. A.* **2006**, *103*, 13872.